

Raman Response of Magnetic Excitations in Cuprate Ladders and Planes

K.P. Schmidt^{1,*} and A. Gössling²

¹*Institut für Theoretische Physik, Universität zu Köln, Zülpicher Str. 77, D-50937 Köln, Germany*

²*II. Physikalisches Institut, Universität zu Köln, Zülpicher Str. 77, D-50937 Köln, Germany*

U. Kuhlmann and C. Thomsen

Institut für Festkörperphysik, Technische Universität Berlin, Hardenbergstr. 36, D-10623 Berlin, Germany

A. Löffert, C. Gross, and W. Assmus

Physikalisches Institut, J.W. Goethe-Universität, Robert-Mayer-Str. 2-4, D-60054 Frankfurt a. M., Germany

(Dated: December 2, 2024)

An unified picture for the Raman response of magnetic excitations in cuprate spin-ladder compounds is obtained by comparing calculated two-triplon Raman line-shapes with those of the prototypical compounds SrCu_2O_3 (Sr123), $\text{Sr}_{14}\text{Cu}_{24}\text{O}_{41}$ (Sr14), and $\text{La}_6\text{Ca}_8\text{Cu}_{24}\text{O}_{41}$ (La6Ca8). The theoretical model for the two-leg ladder contains Heisenberg exchange couplings J_{\parallel} and J_{\perp} plus an additional four-spin interaction J_{cyc} . Within this model Sr123 and Sr14 can be described by $x := J_{\parallel}/J_{\perp} = 1.5$, $x_{\text{cyc}} := J_{\text{cyc}}/J_{\perp} = 0.2$, $J_{\perp}^{\text{Sr123}} = 1130 \text{ cm}^{-1}$ and $J_{\perp}^{\text{Sr14}} = 1080 \text{ cm}^{-1}$. The couplings found for La6Ca8 are $x = 1.2$, $x_{\text{cyc}} = 0.2$, and $J_{\perp}^{\text{La6Ca8}} = 1130 \text{ cm}^{-1}$. The unexpected sharp two-triplon peak in the ladder materials compared to the undoped two-dimensional cuprates can be traced back to the anisotropy of the magnetic exchange in rung and leg direction. With the results obtained for the isotropic ladder we calculate the Raman line-shape of a two-dimensional square lattice using a toy model consisting of a vertical and a horizontal ladder. A direct comparison of these results with Raman experiments for the two-dimensional cuprates R_2CuO_4 ($\text{R}=\text{La},\text{Nd}$), $\text{Sr}_2\text{CuO}_2\text{Cl}_2$, and $\text{YBa}_2\text{Cu}_3\text{O}_{6+\delta}$ yields a good agreement for the dominating two-triplon peak. We conclude that short range quantum fluctuations are dominating the magnetic Raman response in both, ladders and planes. We discuss possible scenarios responsible for the high-energy spectral weight of the Raman line-shape, i.e. phonons, the triple-resonance and multi-particle contributions.

PACS numbers: 75.40.Gb, 75.50.Ee, 75.10.Jm

I. INTRODUCTION

Strongly correlated electron systems in low dimensions are of fundamental interest due to their fascinating properties resulting from strong quantum fluctuations^{1,2,3}. Especially in the case of the high- T_c cuprate superconductors, the role of quantum fluctuations is heavily debated. Two-magnon Raman scattering has been proven to be a powerful tool to study quantum fluctuations in the magnetic sector^{4,5,6,7,8,9}. In contrast to the well understood magnon dispersion as measured by inelastic neutron scattering^{10,11,12,13,14}, the quantitative understanding of the two-magnon line-shape in the Raman response^{5,6} and in the optical conductivity^{15,16,17,18} remains an issue open to debate.

Interestingly, in the so-called cuprate ladder systems like Sr123 or the telephone-number compounds $(\text{Sr,Ca,La})_{14}\text{Cu}_{24}\text{O}_{41}$ a prominent peak in the magnetic Raman response is observed at the same energy of about 3000 cm^{-1} as in the two-dimensional compounds^{19,20,22,23}. In contrast to the gapless long-range ordered two-dimensional compound, the quasi one-dimensional two-leg ladders are known to be realizations of a gapped spin liquid²¹. Because the elementary excitations above this groundstate are triplons²⁴, we call the corresponding Raman response as two-triplon Raman scattering.

On the one hand, one may expect that the Raman response is dominated by short-range, high-energy ex-

citations, suggesting a certain similarity between ladders and planes, both being built from edge-sharing Cu_4 plaquettes. The peak frequencies are in fact at 3000 cm^{-1} . On the other hand, the line shape and in particular the peak width strongly varies between different compounds. In 2D, the peak width is of the order of 1000 cm^{-1} , in La6Ca8 about 500 cm^{-1} , in Sr123 and Sr14 only $(100 - 200) \text{ cm}^{-1}$. Due to the observation of a very sharp two-triplon Raman line in the spin liquid Sr14, Gozar *et al.* have questioned whether the large line width in 2D and the related, heavily discussed spectral weight above the two-magnon peak can be attributed to quantum fluctuations²⁰.

In the last years theoretical developments in the field of quasi one-dimensional systems, namely the quantitative calculation of spectral densities^{25,26,27,28,29,30,31}, has led to a deeper understanding of magnetic contributions to the Raman response of undoped cuprate ladders. Besides the usual Heisenberg exchange terms the minimal magnetic model includes four-spin interactions which are 4-5 times smaller than the leading Heisenberg couplings^{19,27,28,32,33}. The existence and the size of the four-spin interactions are consistent with theoretical derivations of generalized t - J models from one-band or three-band Hubbard models^{34,35,36,37,38,39,40}.

In the present paper we show that the strong variation of the line width can be traced back to changes of the spatial anisotropy of the exchange constants. The sharp Raman line in Sr14 and Sr123 results from $x = 1.5$, the increased line width in La6Ca8 reflects $x = 1.2$, and the

isotropic coupling $x = 1$ for the square lattice yields the much larger width observed in 2D. In fact, we obtain a quantitative description of the dominant Raman peak in 2D using a toy model which mimics the 2D square lattice by the superposition of a vertical and a horizontal ladder. We thus conclude that the dominant Raman peak is well described by short-range excitations.

Besides the dominant two-triplon peak, the large spectral weight measured at high energies remains an open problem for the cuprate ladders and planes. We review possible sources of the high-energy spectral weight which were suggested in the past, e.g. quantum fluctuations^{26,41,42,43,44,45}, the role of spin-phonon interaction^{4,46,47,48,49,50,51} and the triple resonance^{5,52,53,54}. We find that in the case of the cuprate ladders the spin-phonon coupling and triple resonance can be ruled out as a source of the high-energy spectral weight.

II. MODEL

In Raman scattering multi-particle excitations with zero change of the total spin can be measured. Starting at $T = 0$ from an $S = 0$ ground state the singlet excitations with combined zero momentum are probed. The Raman response in spin ladders has been calculated by first order perturbation theory⁵⁵ and by exact diagonalization⁵⁶. In this work, Raman line-shapes are presented obtained from continuous unitary transformations (CUT) using rung triplons as elementary excitations^{26,32}. The results are not resolution limited because neither finite size effects occur nor an artificial broadening is necessary.

For zero hole doping, the minimum model for the magnetic properties of the $S = 1/2$ two-leg ladders is an antiferromagnetic Heisenberg Hamiltonian plus a cyclic four-spin exchange term H_{cyc} ^{27,57,58}

$$H = J_{\perp} \sum_i \mathbf{S}_{1,i} \mathbf{S}_{2,i} + J_{\parallel} \sum_{i,\tau} \mathbf{S}_{\tau,i} \mathbf{S}_{\tau,i+1} + H_{\text{cyc}} \quad (1a)$$

$$H_{\text{cyc}} = J_{\text{cyc}} \sum_i K_{(1,i),(2,i),(2,i+1),(1,i+1)} \quad (1b)$$

$$K_{(1,1),(1,2),(2,2),(2,1)} = K_{1234} = (\mathbf{S}_1 \mathbf{S}_2)(\mathbf{S}_3 \mathbf{S}_4) + (\mathbf{S}_1 \mathbf{S}_4)(\mathbf{S}_2 \mathbf{S}_3) - (\mathbf{S}_1 \mathbf{S}_3)(\mathbf{S}_2 \mathbf{S}_4) \quad (1c)$$

where i denotes the rungs and $\tau \in \{1, 2\}$ the legs. The exchange couplings along the rungs and along the legs are denoted by J_{\perp} and J_{\parallel} , respectively. The relevant couplings modeling Sr123 and Sr14⁵⁹ are illustrated in Fig. 1. There is also another way to include the leading four-spin exchange term by cyclic permutations^{27,33} which differs in certain two-spin terms from Eq. (1)³³. Both Hamiltonians are identical except for couplings along the diagonals if J_{\perp} and J_{\parallel} are suitably redefined⁶¹.

At $T = 0$ the Raman response $I(\omega)$ is given by the retarded resolvent

$$I(\omega) = -\frac{1}{\pi} \text{Im} \langle 0 | \mathcal{O}^{\dagger}(\omega - H + i\delta)^{-1} \mathcal{O} | 0 \rangle. \quad (2)$$

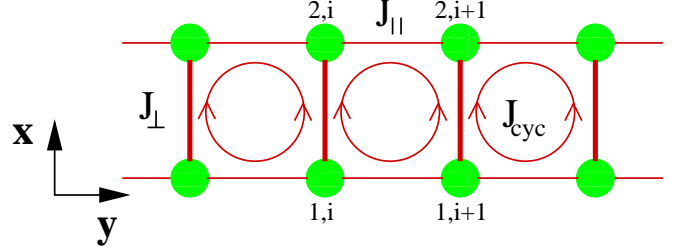


FIG. 1: Schematic view of a two-leg ladder (notation as in Eq. (1)). The circles denote the positions of Cu^{2+} ions carrying a spin $1/2$ each. The crystallographic axes are such that $x \parallel b$ and $y \parallel a$ for Sr123 and $x \parallel a$ and $y \parallel c$ for Sr14.

The observables $\mathcal{O}^{\text{rung}}$ (\mathcal{O}^{leg}) for magnetic light scattering in rung-rung (leg-leg) polarization read in leading order^{62,63}

$$\mathcal{O}^{\text{leg}} = A_0^{\text{leg}} \sum_i (\mathbf{S}_{1,i} \mathbf{S}_{1,i+1} + \mathbf{S}_{2,i} \mathbf{S}_{2,i+1}) \quad (3a)$$

$$\mathcal{O}^{\text{rung}} = A_0^{\text{rung}} \sum_i \mathbf{S}_{1,i} \mathbf{S}_{2,i}. \quad (3b)$$

The factors A_0^{leg} and A_0^{rung} depend on the underlying microscopic electronic model. It is beyond the scope of the present work to compute them. The results will be given in units of these factors squared. In this article we will only consider non-resonant Raman excitation processes. We discuss which laser energy should be used in order to investigate the non-resonant regime.

III. METHOD

Technically, we employ a CUT to map the Hamiltonian H to an effective Hamiltonian H_{eff} which conserves the number of rung-triplons, i.e. $[H_0, H_{\text{eff}}] = 0$ where $H_0 := H|_{\{J_{\parallel}=0; J_{\text{cyc}}=0\}}$ ^{64,65,66}. The ground state of H_{eff} is the rung-triplon vacuum. For the response function $I(\omega)$ the observable \mathcal{O} is mapped to an effective observable \mathcal{O}_{eff} by the same CUT. The CUT is implemented in a perturbative fashion in $x = J_{\parallel}/J_{\perp}$ and $x_{\text{cyc}} = J_{\text{cyc}}/J_{\perp}$. The effective Hamiltonian is calculated up to high orders (1-triplon terms: 11th, 2-triplon terms: 10th order). The effective observable \mathcal{O}_{eff} is computed to order 10 in the 2-triplon sector.

The resulting plain series are represented in terms of the variable $1 - \Delta^{\text{SG}}/(J_{\parallel} + J_{\perp})$ ^{67,68} where Δ^{SG} is the one-triplon gap. Then standard Padé extrapolants⁶⁹ yield reliable results up to $J_{\parallel}/J_{\perp} = 1 - 1.5$ depending on the value of J_{cyc}/J_{\perp} . Consistency checks were carried out by extrapolating the involved quantities before and after Fourier transforms. In case of inconclusive extrapolants the bare truncated series are used. We will estimate the overall accuracy below by comparing with DMRG results²⁷. The Raman line shape is finally calculated as continued fraction by tridiagonalization of the effective two-triplon Hamiltonian.

Sectors with odd number of triplons are inaccessible by Raman scattering due to the invariance of the two observables $\mathcal{O}_{\text{eff}}^{\text{leg}}$ and $\mathcal{O}_{\text{eff}}^{\text{rung}}$ with respect to reflections about the centerline of the ladder²⁶. Thus only excitations with even number of triplons matter. Therefore the leading contributions to the Raman response come from the 2-triplon sector. It was shown earlier that the two-triplon contribution is the dominant part of the Raman response at low and intermediate energies^{26,70}. The role of the four-triplon contribution for the high-energy spectral weight will be discussed at the end of this work.

IV. CUPRATE LADDERS

In this part we will compare the theoretically obtained two-triplon contributions to the experimental line-shapes of the cuprate ladders Sr123 and Sr14. The crystals of Sr123 have been grown and measured under the same conditions as described in Refs. 71 and 19, while the data of Sr14 have been provided by Gozar *et al.*²⁰. The experimental Raman line-shape depends strongly on the laser energy because resonant contributions are present. This becomes apparent in a strong anisotropy between the width of the two-triplon peak in leg and rung polarization for laser energies $\omega_{\text{exc}} = 2-3$ eV. The width of the two-triplon peak in leg polarization is much sharper. For laser energies $\omega_{\text{exc}} < 2$ eV, the strong anisotropy between both polarizations vanishes²⁰. It is therefore important to figure out which laser energy has to be used for the comparison between the non-resonant theory and the experiment in order to study the magnetic excitations only.

The first criterion can be gained from the optical conductivity as for example given in Ref. 20: the intensity of the two-triplon peak develops in the same way as the optical conductivity. For the non-resonant regime both, energy of the incident and scattered light, should be smaller than the charge transfer gap (Sr14: $\Delta_{T=10\text{K}} \sim 2.1$ eV). Thus, we have chosen spectra with laser energies $\omega_{\text{exc}} = 1.92$ eV in the case of Sr14 and $\omega_{\text{exc}} = 1.95$ eV for Sr123. Luckily, the value of the optical conductivity is about $100 \Omega^{-1}\text{cm}^{-1}$ in the sub gap regime at $\omega = \omega_{\text{exc}} - E_{2\text{T}} \sim 1.5$ eV²⁰ (which is 1-2 orders of magnitude larger than for the 2D cuprates⁷²) yielding a non vanishing intensity of the two-triplon peak. Here $E_{2\text{T}}$ denotes the energy of the two-triplon peak.

The second criterion arises from the polarization dependence of the two-triplon peak. Depending on the laser energy used one can observe a drastic difference in the line shape between the two polarizations^{19,20}. While the difference in the line shapes is large for $\omega_{\text{exc}} > 2.1$ eV, it does almost vanish in the case of $\omega_{\text{exc}} < 2.0$ eV²⁰. This fits very well to the weak polarization dependence of the purely magnetic response as described by Eqs. (3): for $x_{\text{cyc}} = 0.0$ the Raman line-shape is identical in the rung and the leg polarization. Small deviations $x_{\text{cyc}} = 0.2$ as relevant for the description of Sr123 and Sr14 produce small deviations with respect to the symmetry between the rung and leg polarization of the ladder. These deviations cannot account for the drastic change between

the two polarizations as observed for $\omega_{\text{exc}} > 2.1$ eV^{19,20}. We therefore conclude that the spectra $\omega_{\text{exc}} < 2.0$ eV are the best choice in order to compare to a purely magnetic, non-resonant theory.

Now we discuss the dependence of the width of the two-triplon peak on the parameters x and x_{cyc} . In Fig. 2, the full width at half maximum (FWHM) of the two-triplon peak is shown. The overall uncertainty shown as error bars in Fig. 2 of the extrapolated two-triplon FWHM was determined by comparing to DMRG data⁷³.

Let us first consider the case $x_{\text{cyc}} = 0.0$. Here the two-triplon width should be identical in both polarizations. It can be clearly seen that the numerically obtained results reflect this property rather well indicating that the uncertainties in the extrapolation are small concerning the matrix elements. There is a strong dependence of the FWHM of the two-triplon peak on the parameter x . The peak sharpens significantly when the ratio x of the magnetic Heisenberg exchanges increases (4 times from $x = 1$ to $x = 1.5$). In the case of $x_{\text{cyc}} \neq 0$, the width depends on the polarization. In general, the width in (xx)-polarization is larger than in (yy)-polarization. For fixed x the FWHM changes at maximum by a factor of two when varying x_{cyc} from 0 to 0.2.

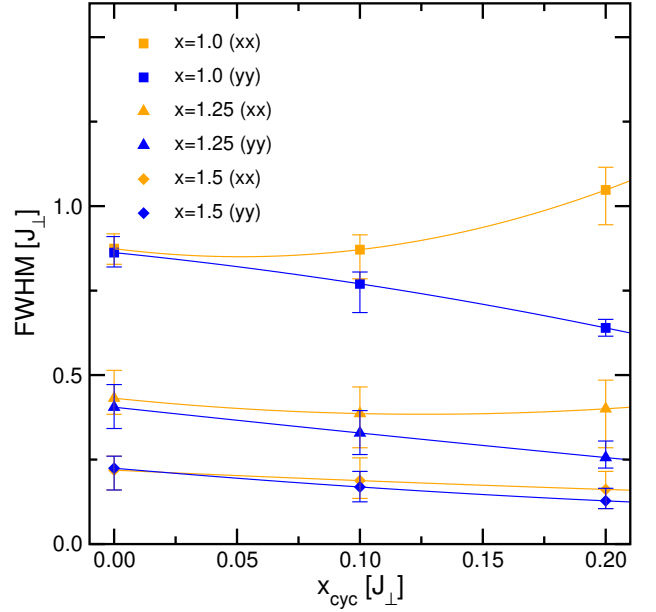


FIG. 2: *Color online* The FWHM of the two-triplon peak for $x := J_{\parallel}/J_{\perp} = 1$ (squares), $x = 1.25$ (triangles) and $x = 1.5$ (diamonds) as a function of the strength of the four-spin interactions $x_{\text{cyc}} := J_{\text{cyc}}/J_{\perp}$. The Orange (Grey) symbols denote (xx)-polarization and the blue (black) symbols (yy)-polarization. The solid lines are a guide to the eye obtained by spline interpolation.

In Figs. 3(a-d), the experimental Raman response of Sr123 and Sr14 is shown for (xx)- and (yy)-polarization (red/black and cyan/grey curves). The spectra of Sr123 were taken in the same way as described in Ref. 19. The data of Sr14 has been made available by Gozar *et al.*²⁰. In addition, theoretically obtained two-triplon contribu-

tions are displayed (orange/grey and blue/black). Experimentally, the width of the two-triplon peak of both materials is almost identical ($\sim 150 \text{ cm}^{-1}$). Only the position of the two-triplon peak is different ($\sim 3140 \text{ cm}^{-1}$ for Sr123 and $\sim 3000 \text{ cm}^{-1}$ for Sr14) which is a result of the slightly different Madelung potentials of both compounds.

For modeling the Raman response we assume $x_{\text{cyc}} = 0.2$ for both compounds. This order of magnitude was previously obtained for cuprate ladders by inelastic neutron scattering^{57,58}, by infrared absorption^{27,28}, Raman response^{19,32} and theoretical works deriving extended low-energy Heisenberg models^{35,74}. In order to account for the FWHM and the two-triplon peak position we determine $x = 1.5$ and global energy scales $J_{\perp} = 1130 \text{ cm}^{-1}$ for Sr123 and $J_{\perp} = 1080 \text{ cm}^{-1}$ for Sr14. It was previously argued that in Sr14 a charge order of the chain subsystem modulates the magnetic exchange in the ladders³². This opens a gap in the Raman response which has a large effect on the two-triplon peak for the parameters $x = 1.2$ and $x_{\text{cyc}} = 0.2$ which are appropriate for La6Ca8. However, the effect is small for larger x -values because the induced gap opens well above the two-triplon peak at $\sim 3600 \text{ cm}^{-1}$. The set of parameters used above for Sr123 and Sr14 describes quantitatively well the Raman response as shown in Tab. I and Figs. 3(a-d). Especially both polarizations for each material can be modeled using only one set of parameters J_{\perp} , x and x_{cyc} . The smaller FWHM of Sr123 and Sr14 compared to La6Ca8^{23,32} can be directly explained by their larger x -values (see Fig. 2). The coupling constants of Sr14 are in good agreement with those obtained by IR absorption measurements⁷⁵. Additionally, our set of parameters yields a spin gap of 290 cm^{-1} for Sr123 and 280 cm^{-1} for Sr14 using the underlying one-triplon dispersion. The latter value is consistent with the spin gap measured by inelastic neutron scattering⁷⁶.

V. CUPRATE PLANES

In this section we calculate the Raman response for the undoped two-dimensional cuprate compounds using a toy model consisting of two uncoupled two-leg ladders (see Fig. 4). This is motivated by the fact that the building blocks of ladders and planes are edge-sharing Cu₄ plaquettes. We expect that the Raman response is dominated by short-range and high-energy excitations yielding a certain similarity between ladders and planes. Indeed, the positions of the two-magnon peak in the 2D cuprates and the two-triplon peak in the cuprate ladders are found at almost the same frequency $\sim 3000 \text{ cm}^{-1}$, but the FWHM of the two-dimensional compounds is a factor of 2-6 larger. We have shown in the last section that the FWHM of the two-triplon peak in the cuprate ladder compounds strongly varies with x . We therefore conjecture that the larger FWHM of the two-dimensional cuprates originates from the isotropic coupling $x = 1$. There will be of course deviations at small energies resulting from the differences between a gapped two-leg

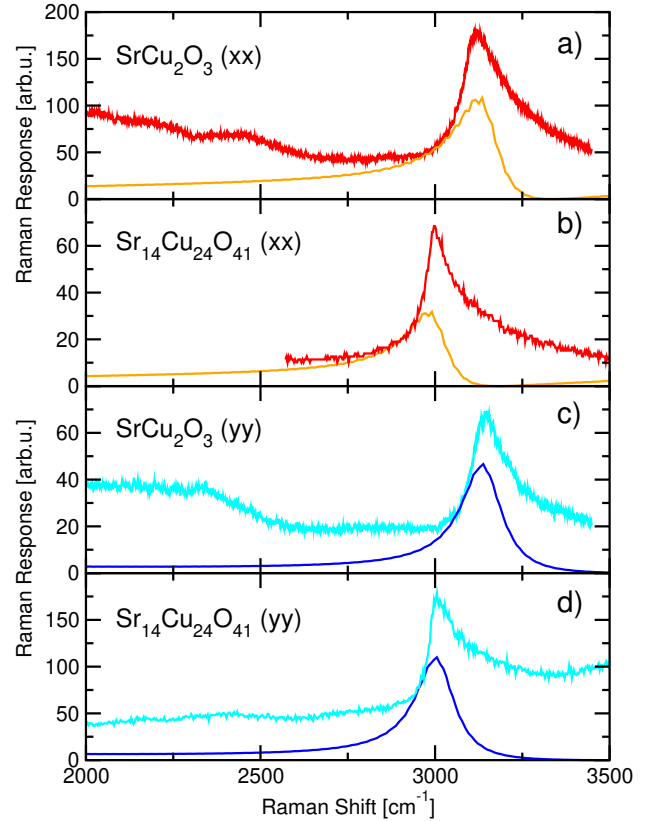


FIG. 3: *Color online* Comparison of the magnetic Raman response of Sr123 ($T = 25 \text{ K}$) and Sr14 ($T = 5 \text{ K}$) with the theoretically obtained two-triplon contribution. The data of Sr14 have been provided by Gozar *et al.*²⁰. (a) The red (black) curve denotes the (xx)-polarization ($x \parallel b$) of Sr123 with a laser excitation energy $\omega_{\text{exc}} = 1.95 \text{ eV}$. The orange (grey) curve displays the theoretical two-triplon contribution with $x = 1.5$, $x_{\text{cyc}} = 0.2$ and $J_{\perp} = 1130 \text{ cm}^{-1}$. (b) The red (black) curve denotes the (xx)-polarization ($x \parallel a$) of Sr14 with a laser excitation energy $\omega_{\text{exc}} = 1.92 \text{ eV}$. The orange (grey) curve displays the theoretical two-triplon contribution with $x = 1.5$, $x_{\text{cyc}} = 0.2$ and $J_{\perp} = 1080 \text{ cm}^{-1}$. (c) (yy)-polarization ($y \parallel a$) for Sr123. Identical parameters as in (a). The cyan (grey) curve displays the experimental data and the blue (black) curve the theoretical two-triplon contribution. (d) (yy)-polarization ($y \parallel c$) for Sr14. Identical parameters as in (b) and the same colors as in (c).

ladder and the gapless excitations in the two-dimensional compounds.

In the following we will show how to deduce the A_{1g} and B_{1g} Raman spectra of the square lattice from those of the two-leg ladder. Clearly, one should use $x = 1$ because the square lattice is isotropic ($J = J_{\parallel} = J_{\perp}$). Starting from the Fleury-Loudon operator the observables $\mathcal{O}^{\text{B}1g}$ ($\mathcal{O}^{\text{A}1g}$) for magnetic light scattering in B_{1g} (A_{1g}) polarization read in leading order for the two-dimensional

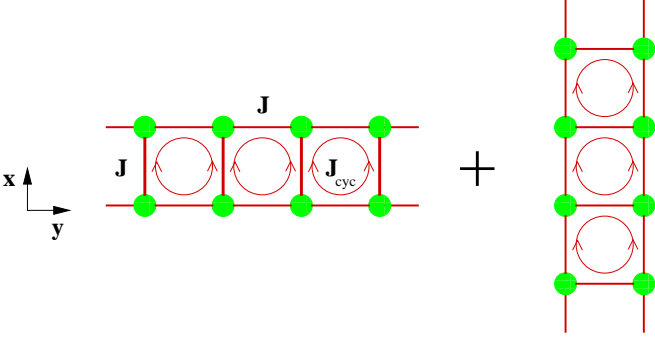


FIG. 4: Sketch of two uncoupled spin-ladders. Here one ladder is oriented in y -direction and the other in x -direction. We approximate the two-dimensional square lattice by the sum of these two uncoupled orthogonal ladders.

square lattice^{62,63}

$$\mathcal{O}^{B1g} = A_{0,B1g} \left(\sum_{\langle ij \rangle, x} \mathbf{S}_i \mathbf{S}_j - \sum_{\langle ij \rangle, y} \mathbf{S}_i \mathbf{S}_j \right) \quad (4a)$$

$$\mathcal{O}^{A1g} = A_{0,A1g} \left(\sum_{\langle ij \rangle, x} \mathbf{S}_i \mathbf{S}_j + \sum_{\langle ij \rangle, y} \mathbf{S}_i \mathbf{S}_j \right) \quad (4b)$$

Here $\langle ij \rangle, x$ ($\langle ij \rangle, y$) denotes a summation over nearest-neighbors in x -direction (y -direction). We approximate the two-dimensional square lattice by a sum of two uncoupled two-leg ladders, one oriented in x -direction, the other in y -direction. The situation is sketched in Fig. 4. The summation over both ladder orientations will restore the square lattice symmetries. Comparing Eq. (4) with Eq. (3) one readily deduces the following relations

$$\mathcal{O}^{B1g} \propto (\mathcal{O}^{\text{leg}} - \mathcal{O}^{\text{rung}}) \quad (5a)$$

$$\mathcal{O}^{A1g} \propto (\mathcal{O}^{\text{leg}} + \mathcal{O}^{\text{rung}}) \quad (5b)$$

between the relevant observables in the two-leg ladder and the two-dimensional square lattice. Note that for $x_{\text{cyc}} = 0$, the Raman response in the A_{1g} polarization vanishes due to the property $\mathcal{O}^{\text{leg}}|0\rangle = -\mathcal{O}^{\text{rung}}|0\rangle$ ²⁶. The latter point is consistent with earlier treatments of the two-dimensional Raman response. But for a finite strength of the four-spin interactions x_{cyc} , also the A_{1g} polarization is finite^{43,46}.

The theoretical two-triplon contribution of the B_{1g} (panel a) and the A_{1g} (panel b) polarization is shown in Fig. 5. The parameters used are an isotropic coupling $x = 1$ and a strength of the four-spin interactions $x_{\text{cyc}} = 0.0$, $x_{\text{cyc}} = 0.1$, and $x_{\text{cyc}} = 0.2$.

The B_{1g} polarization displays a symmetric two-triplon peak which is dominating the Raman response. The four-spin interactions shift the whole spectrum to lower energies and decrease the total intensity. The FWHM of the two-triplon peak is approximately given by the average

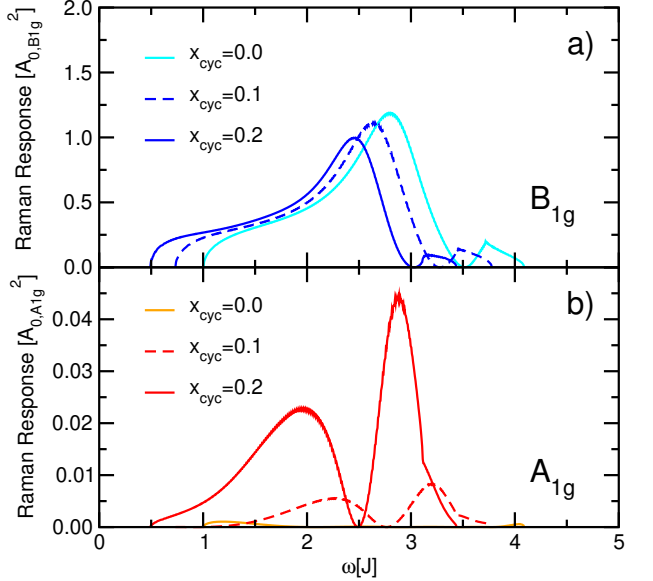


FIG. 5: *Color online* Two-triplon Raman response of the 2D square lattice for $x = 1$. (a) B_{1g} -polarization for $x_{\text{cyc}} = 0.0$ (cyan/grey), $x_{\text{cyc}} = 0.1$ (dashed) and $x_{\text{cyc}} = 0.2$ (blue/black). (b) A_{1g} -polarization for $x_{\text{cyc}} = 0.0$ (orange/grey), $x_{\text{cyc}} = 0.1$ (dashed) and $x_{\text{cyc}} = 0.2$ (red/black). Note the different scales for the Raman response in A_{1g} and B_{1g} spectra.

width of the two-triplon peaks of an isolated two-leg ladder in rung and in leg polarization. Thus, the width is nearly independent of the value of x_{cyc} .

The A_{1g} polarization is almost zero for vanishing x_{cyc} . This again reflects the accurate extrapolation of the matrix elements. For non-zero x_{cyc} , a finite A_{1g} contribution is realized. The differences in the line-shape between A_{1g} and B_{1g} are a pure effect of different matrix elements. Compared to the two-triplon peak in the B_{1g} polarization the A_{1g} polarization displays a two peak structure where the second peak is sharper and at higher energies.

In the following we will compare the theoretical two-triplon contribution to the Raman response with low temperature experimental data on R_2CuO_4 ($\omega_{\text{exc}} = 2.71$ eV)⁶, $\text{Sr}_2\text{CuO}_2\text{Cl}_2$ ($\omega_{\text{exc}} = 2.73$ eV)⁵, and $\text{YBa}_2\text{Cu}_3\text{O}_{6+\delta}$ ($\omega_{\text{exc}} = 2.71$ eV)⁶ taken from the literature.

As discussed in section IV the laser energy used for the experiment is a crucial issue. Analogous to the ladders one should use spectra of cuprate planes measured with laser energies below the charge gap for comparing to the purely magnetic theoretical response. But it turns out that the optical conductivity is rather low ($\lesssim 10 \Omega^{-1}\text{cm}^{-1}$) below the charge gap Δ which results in a vanishing intensity of the two-magnon peak⁵. An analogous choice of the laser energies below the charge gap as discussed for the cuprate ladders is not possible. Therefore, we used data measured with laser energies $\omega_{\text{exc}} = 2.7$ eV $> \Delta$. At the energy $\omega_{\text{exc}} = 2.7$ eV the optical conductivity is quite smooth and $\omega_{\text{exc}} \neq \Delta \approx (1.7 - 2.0)$ eV^{5,72,77}. Simultaneously $\omega_{\text{exc}} = 2.7$ eV coincides with the triple resonance at $\omega_{\text{res}} \approx \Delta + 8J$. The triple resonance theory predicts two peaks in the Raman response

TABLE I: Comparison of the two-triplon peak between experimental data of different cuprate ladder and plane compounds and the theoretical results.

Material	Peak [cm ⁻¹]	Experiment			Ref.	x	x_{cyc}	Theory (CUT)	
		FWHM ^a [cm ⁻¹]	ω_{exc} [eV]	J_{\perp} [cm ⁻¹]				FWHM [cm ⁻¹]	
SrCu ₂ O ₃ (xx)	3120	150-220	1.96	this work	1.5	0.2	1130	180	
SrCu ₂ O ₃ (yy)	3150	120-180	1.96	this work	1.5	0.2	1130	140	
Sr ₁₄ Cu ₂₄ O ₄₁ (xx)	3000	100-160	1.92	20	1.5	0.2	1080	180	
Sr ₁₄ Cu ₂₄ O ₄₁ (yy)	3000	120 ^b	1.92	20	1.5	0.2	1080	140	
La ₆ Ca ₈ Cu ₂₄ O ₄₁ (xx)	3010	550 ^b	2.41	23,32	1.2	0.2	1130	580	
La ₆ Ca ₈ Cu ₂₄ O ₄₁ (yy)	2950	350 ^b	2.41	23,32	1.2	0.2	1130	350	
Sr ₂ CuO ₂ Cl ₂	2950	800-1100	2.73	5	1.0	0.2	1190	1000	
YBa ₂ Cu ₃ O _{6+δ}	2750	1000-1150	2.71	6	1.0	0.2	1110	940	
La ₂ CuO ₄	3170	950-1150	2.71	6	1.0	0.2	1280	1080	
Nd ₂ CuO ₄	2930	900-1050	2.71	6	1.0	0.2	1190	1000	

^a Lower limit of exp. FWHM: linear background subtracted from data. Upper limit: no background corrections.

^b Exp. FWHM: linear background subtracted from data because background exceeds almost the two-triplon peak heights.

at about $2.8J$ and $4J$. The relative intensity of both peaks depends on the laser energy. The second peak is strongly suppressed at ω_{res} . In that sense this laser energy can be assigned to be closest to the non-resonant regime^{52,53,54}.

In Fig. 6 experimental data and theoretical contributions using $x = 1$ and $x_{cyc} = 0.2$ are shown for both polarizations. Frequencies are measured in units of J . We first discuss the B_{1g} polarization in Fig. 6(a). We have chosen the global energy scale J for all experimental curves such that the positions of the experimental two-magnon and the theoretical two-triplon peaks match. This yields quantitatively reasonable values for these compounds. In addition, we find quantitative agreement between the experimental FWHM and the theoretical FWHM of the two-triplon peak. The values of J and the FWHM are listed in Tab. I for all compounds. Note that the FWHM for $x = 1$ is larger than for the anisotropic case $x > 1$ as discussed for the ladder compounds.

Clearly, there are also deviations between theory and experiment. As expected, the low-energy spectral weight in the theoretical line-shape is larger compared to the experimental curves. This is definitely a consequence of approximating the two-dimensional square lattice with quasi one-dimensional models. There is also spectral weight missing at higher energies above the two-triplon peak. Possible explanations will be described below.

The results for the A_{1g} polarization (shown in Fig. 6(b)) are explained next. We used the *same* global energy scales J for the experimental curves as determined from the B_{1g} polarization above. In the experiment a broad hump is measured. We find it very promising that the theoretical contribution displays the dominant spectral weight just for these energies. As expected, the line-shape cannot be resolved completely which we attribute to the simplified modeling of the two-dimensional planes. We conclude that at least a large part of the experimental A_{1g} polarization originates from the finite four-spin interactions. For $x_{cyc} = 0$, there is no purely magnetic contribution to the Raman response for this polarization. A finite A_{1g} Raman response can be regarded as an ev-

idence for the presence of sizable four-spin interactions. This follows entirely from symmetry arguments and holds true for the full two-dimensional model. At higher energies, spectral weight is missing in the theoretical contribution in an analogous fashion as in the B_{1g} polarization.

VI. HIGH-ENERGY SPECTRAL WEIGHT

As shown in Sect. IV and in Sect. V the CUT cannot account for the missing high-energy spectral weight when comparing to the Raman experiments. Also other theories proposed previously like calculations based on spin-waves^{41,42}, paramagnons⁷⁸, Jordan-Wigner fermions⁷⁹ and numerical studies^{26,44,55,56} were faced with the same problem. Extended theories including *(i) multi-particle contribution*, *(ii) spin-phonon coupling*, *(iii) two-magnon/triplon plus phonon absorption* and *(iv) triple resonance* are necessary in order to describe the high-energy spectral weight.

Most of the publications deal with the two-dimensional compounds. Here we will try to review these ideas and reexamine them in the light of our new results. Especially the quantitative results for the cuprate ladders can give new insights in this discussion.

(i) multi-particle contribution One open problem is the role of multi-particle contributions to the Raman response, i.e. the four-magnon contribution in the case of the square lattice and the four-triplon contribution in the case of the two-leg ladder. At this stage no quantitative calculations are available. But it is known that the multi-triplon spectral weights are sizable for the two-leg ladder^{26,70}. The main effect of the four-spin interaction on the high-energy spectral weight is a small shift from the two-triplon to the multi-triplon channels⁷⁰. But this shift is not sufficient to account for the high-energy spectral weight as observed in experiments. This was also found in treatments for the two-dimensional square lattice^{18,43,45}. However, the complete magnetic infrared absorption spectrum (including the high-energy part) of La₆Ca₈ can be described quantitatively by including

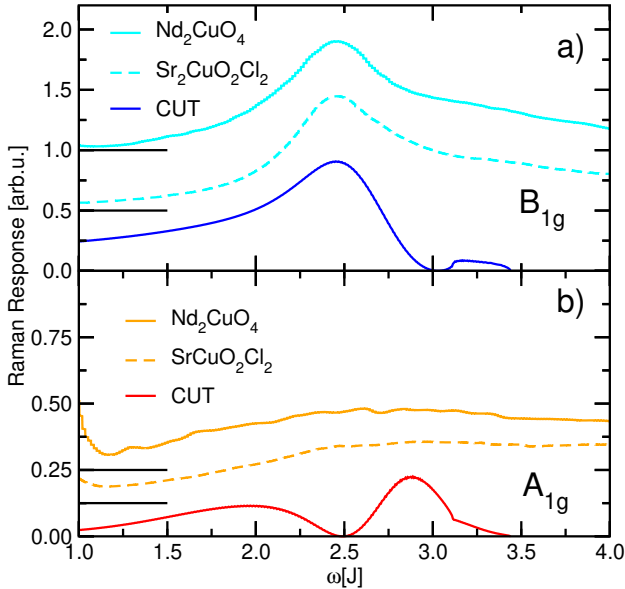


FIG. 6: *Color online* Comparison of the two-triplon Raman response to the two-magnon Raman line-shape of Nd_2CuO_4 ($\omega_{\text{exc}} = 2.71$ eV, $T = 30$ K) and $\text{Sr}_2\text{CuO}_2\text{Cl}_2$ ($\omega_{\text{exc}} = 2.73$ eV, $T = 5$ K). The Raman data of Nd_2CuO_4 and $\text{Sr}_2\text{CuO}_2\text{Cl}_2$ are reproduced from Refs. 6 and 5. The experimental curves are smoothed and their zero position is shifted horizontally as indicated by the black horizontal lines. (a) B_{1g} -polarization: The blue (black) curve denotes the two-triplon contribution with $x = 1$ and $x_{\text{cyc}} = 0.2$. The global energy scale J is chosen such that experimental two-magnon and the theoretical two-triplon peak merge. This yields $J = 1190 \text{ cm}^{-1}$ for Nd_2CuO_4 (cyan/grey) and $\text{Sr}_2\text{CuO}_2\text{Cl}_2$ (dashed). (b) A_{1g} -polarization (theory: red/black; experiment: orange/grey): Same notations as in (a). Note that the *same* magnetic exchange couplings J are used.

multi-particle contributions^{27,28}. Here x_{cyc} does not play the dominant role for the high-energy spectral weight⁸⁰.

It is therefore plausible that these contributions give a noticeable effect also on the high-energy Raman response. There are also indications that the spectral weight cannot be fully explained in this way. For example, the four-magnon spectral weight was shown to be negligible for the 2D square lattice⁴². But the magnon-magnon interaction which was not treated in this calculation could enhance the high-energy spectral weight. Also quantum Monte Carlo calculations which include all magnon contributions for the two-dimensional Heisenberg model seem to explain only a part of the high-energy spectral weight⁴⁴. But finite size effects and inaccuracies of the analytical continuation can lead to uncertainties in determining the high-energy spectral weight.

(ii) *spin-phonon coupling* The latter observations suggest that additional degrees of freedom are important. It was argued by several authors that the coupling to phonons produces a large amount of spectral weight above the two-triplon peak^{4,46,48,49,50,51}. In one approach the spin-phonon coupling modulates the magnetic exchange couplings with a Gaussian distribution. Another

approach introduces a finite spin wave damping induced by the spin-phonon coupling. Both scenarios produce a significantly broadened and asymmetric two-magnon peak as observed in experiments^{50,51}.

Nevertheless, the consistency of a spin-phonon coupling as suggested above with experiments is not clear. The magnitude of this coupling has to be unrealistically large in order to describe infrared absorption data¹⁷. Additionally, it was pointed out by Freitas and Singh⁸¹ that the temperature-dependent correlation length and the spin dynamics which agree well with purely magnetic models does not leave room for such a coupling^{82,83}.

There are no investigations of the role of spin-phonon couplings for the case of the cuprate ladder systems. But the FWHM of the two-triplon peak can be quantitatively understood within a purely magnetic model as shown in Sect. IV. Thus, we conclude that the spin-phonon coupling is not strong in the case of the cuprate ladder compounds. Such a coupling leads to a broad two-triplon peak in the same way as for the two-dimensional case. This is a contradiction when considering the Raman response and the infrared absorption of cuprate ladders simultaneously: on the one hand one needs a larger anisotropy between leg and rung coupling (larger x) in order to sharpen the two-triplon peak in the Raman response again (see Fig. 2) but on the other hand one cannot explain the infrared absorption with an substantially increased x ^{27,75}. A strong spin-phonon coupling is therefore in contradiction with the results obtained for cuprate ladders. This can be also seen as an indication that the same holds true for the two-dimensional compounds⁴.

(iii) *two-magnon/triplon plus phonon absorption* A third alternative explaining the high-energy spectral weight uses phonons as possible momentum sinks. Here a strong spin-phonon coupling is not necessary. The idea is based on the work of Lorenzana and Sawatzky for infrared absorption^{18,84,85}. It is well accepted in the case of infrared absorption measurements on cuprate ladders^{27,80} and planes^{17,18} that the dominant processes are magnetic excitations which are assisted by phonons. It was realized by Freitas and Singh that similar processes could be important also for the Raman response in cuprate planes⁸¹. In an analogous fashion a two-triplon plus (Raman active) phonon process for the Raman response in cuprate ladders could be important. It can be used to transfer spectral weight above the two-triplon peak leading to an asymmetric line-shape. It is a difficult task to determine the relative strength of this process compared to the usual two-triplon scattering.

(iv) *triple resonance* Additionally, the triple resonance was proposed to account for the high-energy spectral weight in the two-dimensional compounds^{5,52,53,54}. As already stated in Sec. V, the experimental spectra of the planes are taken in the resonant regime. It is known that the triple resonance scenario yields an additional peak above the two-magnon peak. Its intensity depends significantly on the energy of the incident light in accordance with experiments⁵. In principle, the same effect is also present in ladder compounds. But for the laser energy $\omega_{\text{exc}} = 1.92$ eV $< \Delta$ considered for Sr123 and Sr14

the triple resonance condition is not fulfilled.

Because a large spin-phonon coupling and the triple resonance can be ruled out for the cuprate ladder systems, the observed high-energy spectral weight in the cuprate ladder compounds has to be explained most probably by the multi-triplon or two-triplon plus phonon contributions.

VII. CONCLUSION

The first part of this work deals with the theoretical understanding of non-resonant magnetic Raman scattering on cuprate two-leg ladder compounds, namely Sr123, Sr14, and La6Ca8. Therefore we applied a triplon-conserving CUT on a microscopic spin-model which includes Heisenberg couplings and additional four-spin interactions. We studied the two-triplon contribution to the non-resonant magnetic Raman response. The dominating feature of the two-triplon contribution is the two-triplon peak which has a characteristic FWHM depending on the model parameters x and x_{cyc} . We carefully chose the experimental data closest to the non-resonant regime and compared them with our theory.

The key observation we found is that the sharpness of the two-triplon peak in Sr123 and Sr14 in comparison to La6Ca8 can be explained by the stronger anisotropy of the magnetic exchange along the rungs and legs of the ladder. Indeed, the two-triplon peak width depends strongly on the parameter x . Both materials can be modeled with the parameters $x \approx 1.5$ and $x_{\text{cyc}} \approx 0.2$ but different global energy scales $J_{\perp} \approx 1130 \text{ cm}^{-1}$ for Sr123 and $J_{\perp} \approx 1080 \text{ cm}^{-1}$ for Sr14. The parameters for Sr14 are in good agreement with infrared absorption^{27,75} and inelastic neutron scattering⁷⁶ experiments. We conclude that the dominating two-triplon peak of the magnetic Raman response in cuprate ladders can be consistently explained within the microscopic model. The presence of a four-spin interaction of the order of $0.2J_{\perp}$ can be viewed as a settled issue.

In the second part of this article we used the results found for the two-leg ladder to describe the magnetic Raman response of the undoped two-dimensional cuprate

compounds in B_{1g} and A_{1g} polarization. The contribution to the A_{1g} polarization is only allowed for finite four-spin interactions due to symmetry reasons. We use an isotropic coupling $x = 1$ and $x_{\text{cyc}} = 0.2$ for the comparison with the experimental data. Convincingly, we find quantitative agreement for the two-triplon peak position *and* the two-triplon peak width for several compounds. Additionally, a sizable spectral weight is found in the A_{1g} polarization consistent with experiments. We conclude that the processes dominating the magnetic Raman response are short-ranged.

The last part deals with the missing high-energy spectral weight above the dominating two-triplon peak for the case of cuprate ladders and planes. We review possible sources of this spectral weight like multi-particle contributions, the role of spin-phonon coupling, a two-triplon plus phonon process and the triple resonance to the magnetic Raman response. We deduced from our results that the high-energy spectral weight cannot be explained with realistic values for the spin-phonon coupling.

In summary, our calculations lead to an unified understanding of the magnetic Raman response in cuprate ladder compounds within a purely magnetic model. A strong spin-phonon coupling can be excluded for these materials. Additionally, we obtained a convincing quantitative description of the dominating two-magnon peak in the Raman response of cuprate planes using a toy model consisting of two uncoupled two-leg ladders. This suggests that the short-ranged triplon excitations might be an alternative starting point for the description of the two-dimensional cuprate compounds.

Acknowledgment

We gratefully acknowledge G.S. Uhrig, M. Grüninger, A. Gozar, A. Reischl, and S. Jandl for very helpful discussions. We thank A. Gozar for the kind provision of experimental data on Sr14. This work is supported by the DFG in SFB 608.

* Electronic address: ks@thp.uni-koeln.de; URL: <http://www.thp.uni-koeln.de/~ks>

¹ J. Orenstein and A.J. Millis, *Science* **288**, 468 (2000).

² S. Sachdev, *Science* **288**, 475 (2000).

³ P.W. Anderson, *Science* **288**, 480 (2000).

⁴ P. Knoll, C. Thomsen, M. Cardona, and P. Murugaraj, *Phys. Rev. B* **42**, 4842 (1990).

⁵ G. Blumberg, P. Abbamonte, M.V. Klein, W.C. Lee, D.M. Ginsberg, L.L. Miller, A. Zibold, *Phys. Rev. B* **53**, R11930 (1996).

⁶ S. Sugai, M. Sato, T. Kobayashi, J. Akimitsu, T. Ito, H. Takagi, S. Uchida, S. Hosoya, T. Kajitani, and T. Fukuda, *Phys. Rev. B* **42**, 1045 (1990).

⁷ P.E. Sulewski, P.A. Fleury, K.B. Lyons, S-W. Cheong, and

Z. Fisk, *Phys. Rev. B* **41**, 225 (1990).

⁸ P.E. Sulewski, P.A. Fleury, K.B. Lyons, and S-W. Cheong, *Phys. Rev. Lett.* **67**, 3864 (1991).

⁹ M. Yoshida, S. Tajima, N. Koshizuka, S. Tanaka, S. Uchida, and T. Itoh, *Phys. Rev. B* **46**, 6505 (1992).

¹⁰ E. Manousakis, *Rev. Mod. Phys.* **63**, 1 (1991).

¹¹ M.A. Kastner, R.J. Birgeneau, G. Shirane, and Y. Endoh, *Rev. Mod. Phys.* **70**, 897 (1998).

¹² S.J. Clarke, A. Harrison, T.E. Mason, and D. Visser, *Solid State Commun.* **112**, 561 (1999).

¹³ S.M. Hayden, G. Aeppli, R. Osborn, A. D. Taylor, T. G. Perring, S.-W. Cheong, and Z. Fisk, *Phys. Rev. Lett.* **67**, 3622 (1991).

¹⁴ R. Coldea, S.M. Hayden, G. Aeppli, T. G. Perring, C.D.

Frost, T.E. Mason, S.-W. Cheong, and Z. Fisk, Phys. Rev. Lett. **86**, 5377 (2001).

¹⁵ J.D. Perkins, J.M. Graybeal, M.A. Kastner, R.J. Birgeneau, J.P. Falck, and M. Greven Phys. Rev. Lett **71**, 1621 (1993).

¹⁶ J.D. Perkins, R.J. Birgeneau, J.M. Graybeal, M.A. Kastner and D.S. Kleinberg, Phys. Rev. B **58**, 9390 (1998).

¹⁷ M. Grüninger, D. van der Marel, A. Damascelli, A. Erb, T. Nunner, and T. Kopp, Phys. Rev. B **62**, 12422 (2000).

¹⁸ J. Lorenzana, J. Eroles, and S. Sorella, Phys. Rev. Lett. **83**, 5122 (1999).

¹⁹ A. Gößling, U. Kuhlmann, C. Thomsen, A. Löffert, C. Gross and W. Assmus, Phys. Rev. B **67**, 052403 (2003).

²⁰ A. Gozar, G. Blumberg, B.S. Dennis, B.S. Shastry, N. Motoyama, H. Eisaki, and S. Uchida, Phys. Rev. Lett. **87**, 197202 (2001).

²¹ E. Dagotto and T.M. Rice, Science **271**, 618 (1996).

²² Z.V. Popović, M.J. Konstantinović, V.A. Ivanov, O.P. Khuong, R. Gajić, A. Vietkin, and V.V. Moshchalkov, Phys. Rev. B **62**, 4963 (2000).

²³ S. Sugai and M. Suzuki, Phys. Stat. Sol. (b) **215**, 653 (1999).

²⁴ K.P. Schmidt and G.S. Uhrig, Phys. Rev. Lett. **90**, 227204 (2003).

²⁵ C. Knetter, K.P. Schmidt, M. Grüninger, and G.S. Uhrig, Phys. Rev. Lett. **87**, 167204 (2001).

²⁶ K.P. Schmidt, C. Knetter, and G.S. Uhrig, Europhys. Lett. **56**, 877 (2001).

²⁷ T. Nunner, P. Brune, T. Kopp, M. Windt, and M. Grüninger, Phys. Rev. B **66**, 180404 (2002).

²⁸ M. Grueninger, M. Windt, E. Benckiser, T.S. Nunner, K.P. Schmidt, G.S. Uhrig und T. Kopp, Adv.Sol.Stat.Phys. **43**, 95 (2003).

²⁹ W. Zheng, C.J. Hamer, and R.R.P. Singh, Phys. Rev. Lett. **91**, 037206 (2003).

³⁰ K.P. Schmidt, C. Knetter and G.S. Uhrig, Phys. Rev. B **69**, 104417 (2004).

³¹ S. Trebst, H. Monien, C.J. Hamer, Z. Weihong, and R.R.P. Singh, Phys. Rev. Lett. **85**, 4373 (2000).

³² K.P. Schmidt, C. Knetter, M. Grüninger, and G.S. Uhrig, Phys. Rev. Lett. **90**, 167201 (2003).

³³ S. Brehmer, H.-J. Mikeska, M. Müller, N. Nagaosa, and S. Uchida, Phys. Rev. B **60**, 329 (1999).

³⁴ E. Müller-Hartmann and A. Reischl, Eur. Phys. J. B **28**, 173 (2002).

³⁵ Y. Mizuno, T. Tohyama and S. Maekawa, J. Phys. Soc. Jpn **66**, 397 (1997).

³⁶ H.J. Schmidt and Y. Kuramoto, Physica C **167**, 263 (1990).

³⁷ M. Takahashi, J. Phys. C: Sol. State Phys. **10**, 1289 (1977).

³⁸ A. H. MacDonald, S. M. Girvin, D. Yoshioka, Phys. Rev. B **41**, 2565 (1990).

³⁹ M. Roger and J.M. Delrieu, Phys. Rev. B **39**, 2299 (1989).

⁴⁰ A. Reischl, E. Müller-Hartmann, G.S. Uhrig, Phys. Rev. B **70**, 245124 (2004).

⁴¹ R.R.P. Singh, P.A. Fleury, K.B. Lyons, and P.E. Sulewski, Phys. Rev. Lett. **62**, 2736 (1989).

⁴² C.M. Canali and S.M. Girvin, Phys. Rev. B **45**, 7127 (1992).

⁴³ Y. Honda, Y. Kuramoto, and T. Watanabe, Phys. Rev. B **47**, 11329 (1993).

⁴⁴ A.W. Sandvik, S. Capponi, D. Poilblanc, and E. Dagotto, Phys. Rev. B **57**, 8478 (1998).

⁴⁵ A.A. Katanin, and P.A. Kampf, Phys. Rev. B **67**, 100404(R) (2003).

⁴⁶ J. Eroles, C.D. Batista, S.B. Bacci, and E.R. Gagliano, Phys. Rev. B **59**, 1468 (1999).

⁴⁷ M.J. Reilly and A.G. Rojo, Phys. Rev. B **53**, 6429 (1996).

⁴⁸ D.U. Sänger, Phys. Rev. B **52**, 1025 (1995).

⁴⁹ W.H. Weber and G.W. Ford, Phys. Rev. B **40**, 6890 (1989).

⁵⁰ S. Haas, E. Dagotto, J. Riera, R. Merlin, and F. Nori, J. Appl. Phys. **75**, 6340 (1994).

⁵¹ F. Nori, R. Merlin, S. Haas, A. Sandvik, and E. Dagotto, Phys. Rev. Lett. **75**, 553 (1995).

⁵² A.V. Chubukov, and D.M. Frenkel, Phys. Rev. Lett. **74**, 3057 (1995).

⁵³ F. Schönenfeld, A.P. Kampf, and E. Müller-Hartmann, Z. Phys. B **102**, 25 (1997).

⁵⁴ K. Morr and A.V. Chubukov, Phys. Rev. B **56**, 9134 (1997).

⁵⁵ C. Jurecka, V. Grützun, A. Friedrich, and W. Brenig, Eur. Phys. J. B **21**, 469 (2001).

⁵⁶ Y. Natsuma, Y. Watabe and T. Suzuki, Phys. Soc. Japan **67**, 3314 (1998).

⁵⁷ M. Matsuda, K. Katsumata, R.S. Eccleston, S. Brehmer, and H.J. Mikeska, J. Appl. Phys. **87**, 6271 (2000).

⁵⁸ M. Matsuda, K. Katsumata, R.S. Eccleston, S. Brehmer, and H.-J. Mikeska, Phys. Rev. B **62**, 8903 (2000).

⁵⁹ Sr14 has intrinsically six holes per unit cell, but it is believed that the majority of the holes are located in the chain subsystem (see Ref. 60).

⁶⁰ N. Nücker, M. Merz, C. A. Kuntscher, S. Gerhold, S. Schuppler, R. Neudert, M.S. Golden, J. Fink, D. Schild, S. Stadler, V. Chakarian, J. Freeland, Y.U. Idzerda, K. Conder, M. Uehara, T. Nagata, J. Goto, J. Akimitsu, N. Motoyama, H. Eisaki, S. Uchida, U. Ammerahl, and A. Revcolevschi, Phys. Rev. B **62**, 14384 (2000).

⁶¹ Neglecting the two-spin exchange terms along the diagonals, our notation J_{\perp} , J_{\parallel} , J_{cyc} is given in terms of the other notation J_{\perp}^P , J_{\parallel}^P , J_{cyc}^P using cyclic permutations by $J_{\parallel} = J_{\perp}^P + \frac{1}{4}J_{\text{cyc}}^P$, $J_{\perp} = J_{\perp}^P + \frac{1}{2}J_{\text{cyc}}^P$, and $J_{\text{cyc}} = J_{\text{cyc}}^P$ (see Ref. 33).

⁶² P.A. Fleury and R. Loudon, Phys. Rev. **166**, 514 (1968).

⁶³ B.S. Shastry and B.I. Shraiman, Phys. Rev. Lett. **65**, 1068 (1990).

⁶⁴ C. Knetter and G.S. Uhrig, Eur. Phys. J. B **13**, 209 (2000).

⁶⁵ C. Knetter, K.P. Schmidt, and G.S. Uhrig, J. Phys.: Condens. Matter **36**, 7889 (2003).

⁶⁶ C. Knetter, K.P. Schmidt, and G.S. Uhrig, Eur. Phys. J. B **36**, 525 (2004).

⁶⁷ K.P. Schmidt, C. Knetter, and G.S. Uhrig, Acta Physica Polonica B **34**, 1481 (2003).

⁶⁸ K.P. Schmidt, H. Monien, and G.S. Uhrig, Phys. Rev. B **67**, 184413 (2003).

⁶⁹ C. Domb and J.L. Lebowitz, *Phase Transitions and Critical Phenomena*, Academic Press, New York, vol. 13 (1989).

⁷⁰ K.P. Schmidt, PhD thesis, University of Cologne (2004).

⁷¹ A. Löffert, C. Gross, and W. Assmus, J. Cryst. Growth **237**, 796 (2002).

⁷² H.S. Choi, Y.S. Lee, T.W. Noh, E.J. Choi, Y. Bang, and Y.J. Kim Phys. Rev. B **60**, 4646 (1999).

⁷³ The extrapolation of the matrix elements are relatively accurate. The maximum deviation between the two-triplon widths in both polarizations is $0.03J_{\perp}$ for $x_{\text{cyc}} = 0$. The one-triplon hopping elements yield a quantitative one-triplon dispersion when compared to DMRG data (see Ref. 27). So we conclude that the largest extrapolation error is due to the extrapolation of the two-triplon interaction amplitudes. To get an estimate of this error we compared the energy of the $S = 0$ two-triplon bound state at finite momentum for $x_{\text{cyc}} = 0$ obtained by DMRG with

the results of the CUT. Then we changed the two-triplon interaction for the Raman case by the maximum deviation of the bound state energies and calculated the effect on the FWHM of the two-triplon peak. In the end we added $0.03J_{\perp}$ to account for the uncertainty of the matrix elements. The resulting uncertainties are shown as error bars in Fig. 2.

⁷⁴ C.J. Calzado, C. de Graaf, E. Bordas, R. Caballol, and J-P. Malrieu, Phys. Rev. B **67**, 132409 (2003).
⁷⁵ M. Windt, PhD thesis, University of Cologne (2003).
⁷⁶ R.S. Eccleston, M. Uehara, J. Akimitsu, H. Eisaki, N. Motoyama, and S.-I. Uchida, Phys. Rev. Lett. **81**, 1702 (1998).
⁷⁷ D. Salamon, Ran Liu, M.V. Klein, M.A. Karlow, S.L. Cooper, S-W. Cheong, W.C. Lee and D.M. Ginsberg, Phys. Rev. B **51**, 6617 (1995).
⁷⁸ T.C. Hsu, Phys. Rev. B **41**, 11379 (1990).
⁷⁹ Y.R. Wang, Phys. Rev. B **43**, 13774 (1991).
⁸⁰ M. Windt, M. Grüninger, T. Nunner, C. Knetter, K.P.

Schmidt, G.S. Uhrig, T. Kopp, A. Freimuth, U. Ammerahl, B. Büchner, and A. Revcolevschi, Phys. Rev. Lett. **87**, 127002 (2001).

⁸¹ P.J. Freitas and R.R.P. Singh, Phys. Rev. B **62**, 5525 (2000).
⁸² Y. Endoh, K. Yamada, R.J. Birgeneau, D.R. Gabbe, H.P. Jenssen, M.A. Kastner, C.J. Peters, P.J. Picone, T.R. Thurston, M. Tranquada, G. Shirane, Y. Hidaka, M. Oda, Y. Enomoto, M. Suzuki, and T. Murakami, Phys. Rev. B **37**, 7443 (1988).
⁸³ S. Chakravarty, B.I. Halperin, and D.R. Nelson, Phys. Rev. B **39**, 2344 (1989). and B. Dabrowski, Phys. Rev. B **49**, R13295 (1994).
⁸⁴ J. Lorenzana and G.A. Sawatzky, Phys. Rev. Lett. **74**, 1867 (1995).
⁸⁵ J. Lorenzana and G.A. Sawatzky, Phys. Rev. B **52**, 9576 (1995).